Geobios 46 (2013) 273–283

Available online at
SciVerse ScienceDirect
www.sciencedirect.com

Elsevier Masson France
EM|consulte
www.em-consulte.com

Original article

Osteoderm microstructure of "rauisuchian" archosaurs from South America☆

Ignacio Alejandro Cerda [a,b,*], Julia Brenda Desojo [a,c], Torsten M. Scheyer [d], Cesar Leandro Schultz [e]

[a] Consejo Nacional de Investigaciones Científicas y Tecnológicas (CONICET), Argentina
[b] Instituto de Investigación en Paleobiología y Geología, Universidad Nacional de Río Negro, Museo Carlos Ameghino, Belgrano 1700, Paraje Pichi Ruca (predio Marabunta), 8300 Cipolletti, Río Negro, Argentina
[c] Sección Paleontología Vertebrados, Museo Argentino de Ciencias Naturales Bernardino Rivadavia, Ángel Gallardo 470 C1405DJR, Buenos Aires, Argentina
[d] Paläontologisches Institut und Museum der Universität Zürich, Karl Schmid-Strasse 4, CH-8006 Zürich, Switzerland
[e] Instituto de Geociências, UFRGS, Caixa Postal 15.001, CEP 91540-000, Porto Alegre, Brazil

ARTICLE INFO

Article history:
Received 11 August 2012
Accepted 24 January 2013
Available online 30 April 2013

Keywords:
Archosauria
"Rauisuchia"
Microanatomy
Histology
Dermal armour
Osteogenesis

ABSTRACT

In this contribution we analyze and discuss the microanatomy and histology of postcranial osteoderms of a number of "rauisuchians" from different localities of South America (Argentina and Brazil). The studied sample includes osteoderms of *Fasolasuchus tenax*, *Prestosuchus chiniquensis*, *Saurosuchus galilei* and an undetermined rauisuchian from Brazil. The bone microanatomy of the osteoderms is variable: whereas some specimens have a rather compact structure, others show a diploe architecture with a central cancellous core bordered by two compact cortices. Both external and basal cortices are mainly composed of poorly vascularized, fine and coarse parallel-fibred bone and networks of interwoven and mineralized fiber bundles. The internal region of the non-remodeled specimens consists of a well-vascularized core in which the intrinsic fibers exhibit important variations (even in the same specimen), ranging from coarse, parallel-fibred to woven-fibred bone tissues. Lines of arrested growth (LAGs) are well recorded in both basal and external cortices. Differences in the bone microstructure (compact *vs.* diploe) could be related to the age, sex and reproductive status of the sampled individuals. Hence, age estimation based on the count of LAGs in rauisuchian osteoderms appears to be reliable only in the early stages of ontogeny. The bone microstructure suggests that rauisuchian osteoderms were originated through a mechanism that involves both intramembranous and metaplastic ossifications.

1. Introduction

"Rauisuchians" are either considered to be a clade of pseudosuchian archosaurs (Brusatte et al., 2010) or a paraphyletic or polyphyletic group (Gower, 2000; Nesbitt, 2011). Both taxonomically and ecologically diverse, rauisuchians are a group of mainly large terrestrial reptiles that lived during the Early to Late Triassic and are considered the top predators of that age (Gower, 2000; Nesbitt, 2005; Nesbitt et al., in press). This particular group was a characteristic component of Triassic continental ecosystems of Europe, North Africa, India, Asia and the Americas (Gower, 2000). In South America, rauisuchians are represented by *Rauisuchus tiradentes* (Huene, 1938), *Prestosuchus chiniquensis* (Huene, 1938), "*Prestosuchus*" *loricatus* (Huene, 1938), *Decuriasuchus quartacolonia* (França et al., 2011) from Brazil, and *Saurosuchus galilei* (Reig, 1959), *Fasolasuchus tenax* (Bonaparte, 1981) and *Luperosuchus fractus* (Romer, 1971) from Argentina.

As in other lineages of archosauriforms (e.g., Aetosauria and Phytosauria), rauisuchians were osteoderm-bearing reptiles. Rauisuchian "dermal armor" comprises two paramedian rows of osteoderms along the cervical, dorsal and sacral regions, and a median row of caudal osteoderms (Fig. 1(A, B)). In some taxa, a single row of ventral-caudal osteoderms has been also reported (Krebs, 1965; França et al., 2011). All osteoderms imbricate, and show distinctive anterior (overlapped) and posterior (overlapping) regions. The precaudal osteoderms are typically asymmetric elements in sagittal plane, organized in two pairs per vertebra (Fig. 1(C)). Conversely, caudal osteoderms have a symmetrical shape and they are arranged one pair per vertebra (Fig. 1(D, E)).

Compared with other groups of armored archosaurs (e.g., aetosaurs or crocodylians), morphological and histological studies of rauisuchian osteoderms are scarce. The absence of paleohistological studies is rather surprising, because osteoderm microstructure can be used to address several issues, including: osteoderm origin and development (Ricqlès et al., 2001; Scheyer and Sander, 2004, 2009; Scheyer, 2007), osteoderm function (Buffrénil et al., 1986; Dias and Richter, 2002; Farlow et al., 2010;

☆ Corresponding editor: Gilles Escarguel.

* Corresponding author. Instituto de Investigación en Paleobiología y Geología, Universidad Nacional de Río Negro, Museo Carlos Ameghino, Belgrano 1700, Paraje Pichi Ruca (predio Marabunta), 8300 Cipolletti, Río Negro, Argentina.
E-mail address: nachocerda6@yahoo.com.ar (I.A. Cerda).

0016-6995/$ – see front matter © 2013 Elsevier Masson SAS. All rights reserved.
http://dx.doi.org/10.1016/j.geobios.2013.01.004

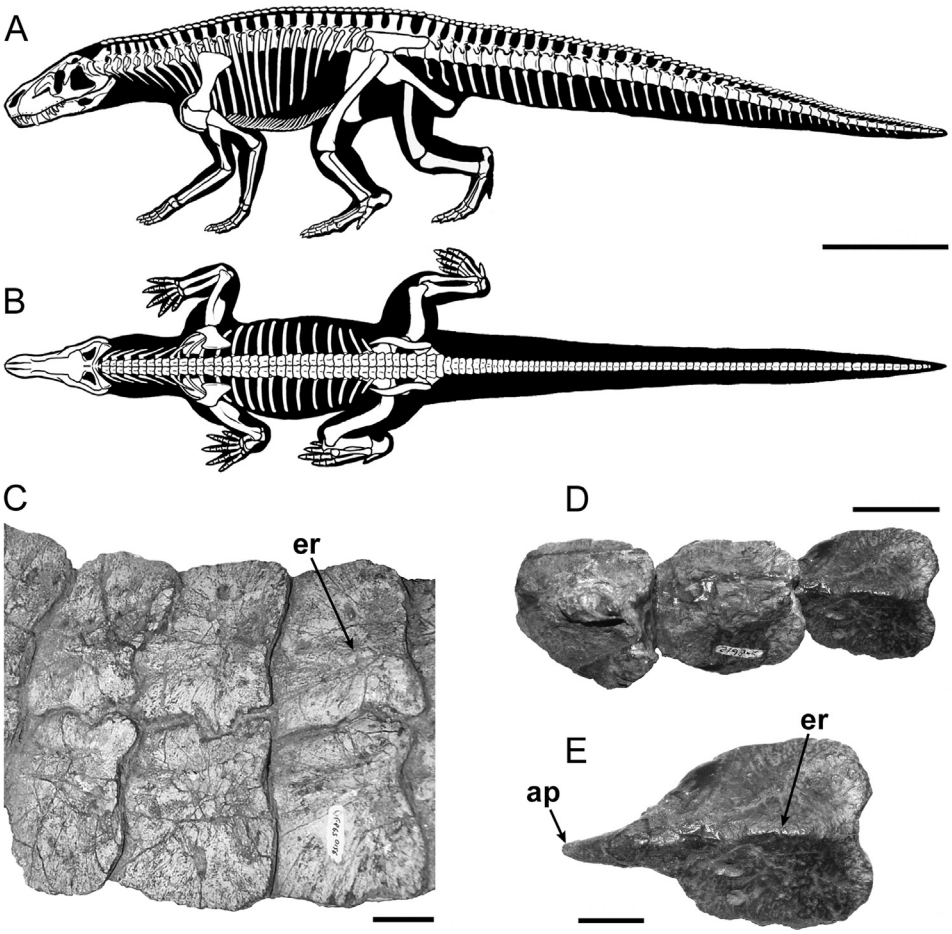

Fig. 1. Morphology and arrangement of "rauisuchian" osteoderms. **A**-**B**. Skeletal reconstruction of *Prestosuchus chiniquensis* in lateral (A) and dorsal (B) views showing the predicted position and arrangement of the osteoderms. **C**. Paired dorsal osteoderms of *P. chiniquensis* (UFRGS-PV0156T) in external view. **D**. Three unpaired, caudal osteoderms of *Saurosuchus galilei* (PVL 2198) in external view. **E**. Caudal osteoderm of the same specimen. Note the development of the anterior projection (ap) and the prominent ridge (er) on the external surface. The anterior end of the osteoderms in pictures C and D is orientated toward the left margin of image. Scale bars: 1 m (A, B), 2 cm (C, D), 1 cm (E).

Hayashi et al., 2010), soft tissue reconstructions (Scheyer and Sander, 2004; Hill, 2006; Cerda and Powell, 2010; Buchwitz et al., 2012), age estimation (Erickson and Brochu, 1999; Cerda and Desojo, 2011), paleoecology (Hua and Buffrénil, 1996; Scheyer and Sander, 2007; Witzmann, 2009), and systematics (Scheyer and Sander, 2004; Burns, 2008; Wolf et al., 2011). To date, the only comprehensive study on the bone microstructure of rauisuchian osteoderms has been carried out by Scheyer and Desojo (2011). In that contribution, rauisuchian osteoderms (including *Batrachotomus kupferzellensis*, *P. chiniquensis*, *"P." loricatus*, *R. tiradentes*, *Ticinosuchus ferox*, *Tikisuchus romeri*, and *Yarasuchus deccanensis*) were characterized as rather compact structures, which usually lacked large bone remodeling or large areas of cancellous bone. The absence of mineralized structural fiber bundles in the core area of the sampled specimens (except for *B. kupferzellensis*) was interpreted as evidence of intramembranous ossification.

In the present study, we analyze and characterize the osteoderm microanatomy and histology of rauisuchian archosaurs from the Middle and Late Triassic of Argentina and Brazil, including *P. chiniquensis*, *F. tenax*, *S. galilei* and an indeterminate rauisuchian (UFRGS-PV-0152-T). The aim of the present contribution is not only to increase the sample size of the previous work of Scheyer and Desojo (2011), but to better understand the probable mode of skeletogenesis of these structures. Also, we evaluate and discuss the possibilities for the usage of osteoderms as a tool in studies of skeletochronology.

2. Material and methods

Precaudal and caudal osteoderms of six rauisuchian individuals were sampled (Fig. 2). Data on accession numbers, locality and horizon of these samples are compiled in Table 1. When the sampled osteoderm was not articulated with elements of the axial skeleton, its topological position along the vertebral column was determined on the basis of the morphology of the element. In some cases, the exact location of the precaudal osteoderms (cervical, dorsal or sacral) could not be identified.

Specimens were prepared for thin sections based on the methodology outlined in Chinsamy and Raath (1992). Given that histology is a destructive method, all specimens were photographed and standard measurements were taken before sectioning. The preparation of the histological sections was carried out in the Departamento de Geología de la Universidad Nacional de San Luis (Argentina). Two transversal thin sections were obtained from each osteoderm; they were analyzed under a light microscope in normal and cross-polarized light conditions, and they are housed at the Coleccion Nacional de Paleovertebrados from the Museo Argentino de Ciencias Naturales Bernardino Rivadavia of Argentina.

The terminology used in this study for describing the various types of osseous tissues refers to Francillon-Vieillot et al. (1990). Regarding the relative location of specific structures within the osteoderm, we use the term "external" to refer the portion of the osteoderm oriented toward the body surface, and "basal" for

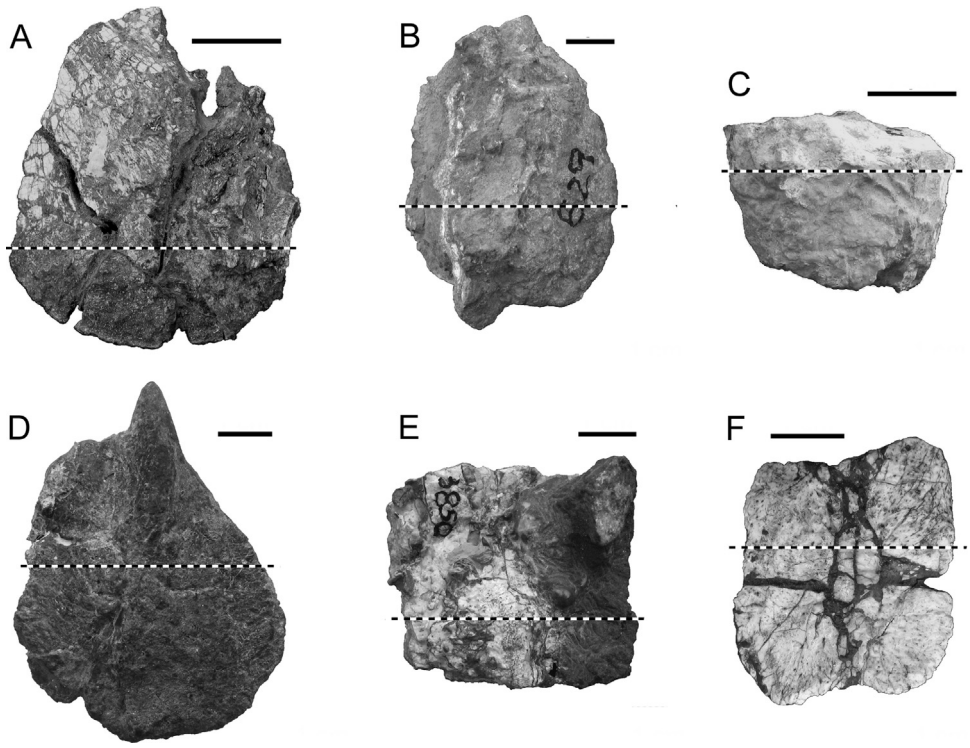

Fig. 2. "Rausuchian" osteoderms sampled in the present study. All elements are in external view, with the anterior edge located toward the top of the picture. Dashed lines indicate the planes of the sections shown in Fig. 3. **A**. *Prestosuchus chiniquensis*, UFRGS-PV0156T. **B**. *P. chiniquensis*, UFRGS-PV0629T. **C**. *P. chiniquensis*, CPEZ-239b. **D**. *Saurosuchus galilei*, PVSJ 32. **E**. *Fasolasuchus tenax*, PVL 3850. **F**. "Rauisuchia" indet., UFRGS-PV-0152-T. Scale bars: 2 cm (A), 1 cm (B–F).

Table 1
"Rauisuchian" osteoderms sectioned for the present study.

Taxon	Specimen number	Locality	Horizon and age	Position
Prestosuchus chiniquensis	UFRGS-PV0156T	Sanga Pascual, Pinheiros, Candelária, Brazil	Santa Maria Fm. (Ladinian)	Precaudal
Prestosuchus chiniquensis	UFRGS-PV0629T	"Posto de Gasolina", Dona Francisca, Brazil	Santa Maria Fm. (Ladinian)	Caudal
Prestosuchus chiniquensis	CPEZ-239b	Sanga da Árvore (Baum Sanga), Sãn Pedro do Sul, Brazil	Santa Maria Fm. (Ladinian)	Cervical
Saurosuchus galilei	PVSJ 32	Valle de la Luna, San Juan, Argentina	Ischigualasto Fm. (Carnian-Norian)	Cervical
Fasolasuchus tenax	PVL 3850	La Esquina, La Rioja, Argentina	Los Colorados Fm. (Late Norian)	Caudal
"Rauisuchia" indet.	UFRGS-PV-0152-T	Railroad cut near General Câmara city	Santa Maria Fm (Ladinian)	Caudal

the portion that is oriented toward the interior of the organism (Scheyer and Sander, 2004). These terms are synonyms of "distal/proximal" (Main et al., 2005) and "superficial/deep" (Hill, 2006, 2010). We use the term "marginal" cortex to refer to the lateral and medial regions of the osteoderms.

3. Results

3.1. General morphology

3.1.1. Prestosuchus chiniquensis (UFRGS-PV0156T)

This osteoderm is part of an individual described by Barberena (1978) and Azevedo (1991) which consists of a complete skull and some cervical, dorsal, and caudal vertebrae. According to its morphology, the osteoderm is from the precaudal region. The element is large (73 mm of the preserved length), strongly concave on its basal surface and dorsally convex (Fig. 2(A)). Observations of other articulated osteoderms from the same individual indicate that the external surface is rather smooth, with shallow grooves that radiate from the highest point of the osteoderms. Also, sub-circular fossae are observable in some elements (Fig. 1(C)). The sampled osteoderm is badly preserved and both external and basal cortices have been almost entirely weathered away.

3.1.2. Prestosuchus chiniquensis (UFRGS-PV0629T)

This sample belongs to the most completely-known specimen of *P. chiniquensis*, which preserves the skull and several appendicular and axial elements, and an articulated series of dorsal osteoderms (Mastrantonio et al., 2008; Mastrantonio, 2010). The analyzed element is a medium-sized (55 mm in length), caudal osteoderm (Fig. 2(B)). Because the specimen is still imbedded in a sedimentary matrix, the surface texture of the external and basal cortices could not be observed. However, other preserved osteoderms of the dorsal series indicate that the external surface is rather smooth, with a similar pattern of radiating, and shallow grooves as observed in the specimen UFRGS-PV0156T. The thin sections reveal that the sample is badly crushed and heavily altered by recrystallization in several regions, obliterating histological details.

3.1.3. Prestosuchus chiniquensis (CPEZ-239b)

This specimen (osteoderm associated with cervical vertebrae and other cervical osteoderms) is part of an incomplete individual that includes cranial and postcranial elements (Lacerda and Schultz, 2010; Lacerda, 2012). Based on size of the specimens UFRGS-PV0156T and UFRGS-PV0629T, Lacerda (2012) considers CPEZ-239b as a juvenile specimen of *P. chiniquensis* (femur lengths of CPEZ-239b and UFRGS-PV0629T are 32.5 and 46.4 cm, respectively). The

Table 2
Synthesis of microanatomical and histological features of the sampled "rauisuchian" osteoderms.

Specimen	Microanatomy	Cortical bone	Internal core	Growth marks
P. chiniquensis UFRGS-PV0156T	Diploe	Avascular. PFB	CB	8
P. chiniquensis UFRGS-PV0629T	Compact	Poorly vascularised. PFB	PFB and WFB	7
P. chiniquensis CPEZ-239b	Compact	Poorly vascularised. PFB	PFB and WFB	5
S. galilei PVSJ 32	Compact	Poorly vascularised. PFB	PFB and WFB	15
F. tenax PVL 3850	Diploe	Well vascularised. PFB	CB, PFB and FLB	8
"Rauisuchia" indet. UFRGS-PV-0152-T	Diploe	Poorly vascularised. PFB	CB, PFB and FLB	8

CB: cancellous bone; FLB: fibrolamellar bone; PFB: parallel-fibred bone; WFB: woven-fibred bone.

sectioned osteoderm is an incomplete element that probably did not exceed 30 mm in total length (Fig. 2(C)); its preservation precludes an accurate morphological description. The external surface is altered, probably due to the acidic preparation of the material (Desojo et al., 2011; Lacerda, 2012). The basal surface is still imbedded in the sediment matrix.

3.1.4. Saurosuchus galilei (PVSJ 32)

The sectioned osteoderm is part of a well-preserved skeleton of *S. galilei*, which consists of a skull and an incomplete postcranium (Alcober, 2000; Trotteyn et al., 2011). The sample consists of a complete, medium-sized (64 mm in length) cervical osteoderm, associated with the fourth cervical vertebra. The specimen is asymmetrical, composed of a medial horizontal and angled lateral portion, which form a thickened ridge at the midline (Fig. 2(D)). The lateral margin is rounded and the medial margin is irregular. The anterior projection is well developed. The basal surface is concave. Both external and basal surfaces are not sculptured and appear smooth.

3.1.5. Fasolasuchus tenax (PVL 3850)

This is an incomplete osteoderm of the holotype of *F. tenax* (Bonaparte, 1981; Fig. 2(E)). Because the sample is broken and partially covered with sediment, its external morphology is only partially observable. A well-developed ridge is present in the posterior region of the external surface. The basal surface is slightly concave. Given that both external and basal surfaces are partially eroded and/or covered with matrix, its surface texture is not visible.

3.1.6. "Rauisuchia" indet. (UFRGS-PV-0152-T)

This osteoderm belongs to an almost complete individual, which is currently under study by one of us (Schultz and Raugust, ongoing work). The element is an incomplete caudal osteoderm (preserved length: 32 mm) whose anterior portion is missing (Fig. 2(F)). The osteoderm possesses a prominent concavity on the posterior region of the basal surface, which contacts the following (posterior) osteoderm in the row. The external surface is smooth, without any sculpturing. The basal surface has a texture of

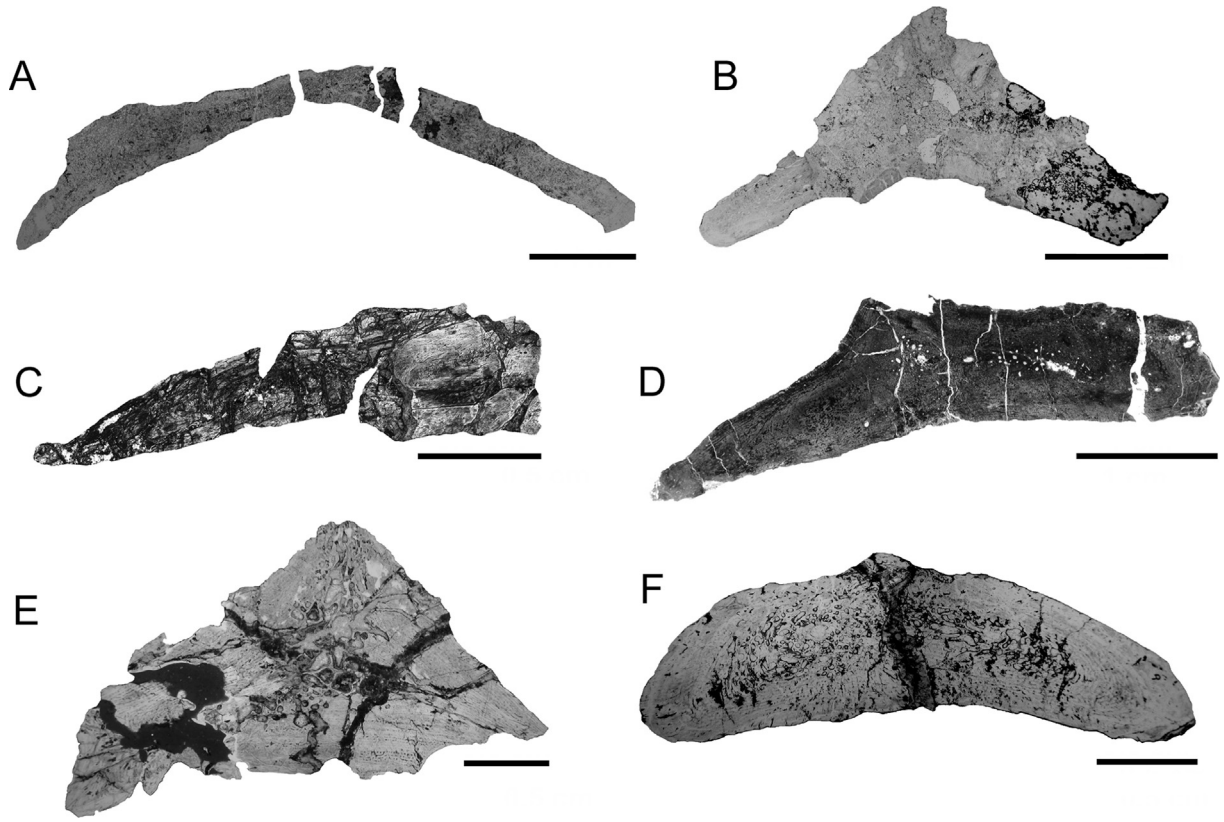

Fig. 3. Transverse sections of different "rauisuchian" osteoderms. **A**. *Prestosuchus chiniquensis*, UFRGS-PV0156T. **B**. *P. chiniquensis*, UFRGS-PV0629T. **C**. *P. chiniquensis*, CPEZ-239b. **D**. *Saurosuchus galilei*, PVSJ 32. **E**. *Fasolasuchus tenax*, PVL 3850. **F**. "Rauisuchia" indet., UFRGS-PV-0152-T. Scale bars: 1 cm (A, B, D), 5 mm (C, E, F).

crisscrossed fibers intersecting like the threads of a woven textile (a common feature on archosauriform osteoderms). Each fiber strut of the crisscrossed texture is aligned, forming an angle of about 45° with the sagittal plane of the element. The marginal edges are irregular in external view.

3.2. Bone microanatomy and histology

The main microanatomical and histological features of rauisuchian osteoderms are synthesized in Table 2. The osteoderms consist of a compact cortex and an internal core, which can be compact or cancellous (Fig. 3). When cancellous bone is present, this tissue appears to be more strongly developed in the mid portion of the osteoderm. The primary bone tissue most commonly reported in the cortical bone is parallel-fibred bone tissue. Other types of primary bone (e.g., woven-fibred bone) can be recorded in the internal core. Sharpey's fibers are commonly observed in the compact bone. Lines of arrested growth (LAGs) are observed in all osteoderms. The principal variation among the sampled osteoderms is in regard to their microanatomy (compact *vs*. diploe), degree of vascularization and number of LAGs.

3.2.1. Bone microanatomy

The microanatomy of the sampled rauisuchian osteoderms is variable (Fig. 3): whereas the specimens PVSJ 32 (*S. galilei*) and UFRGS-PV0629T and CPEZ-239b (*P. chiniquensis*) have compact structures, UFRGS-PV0156T (*P. chiniquensis*), PVL 3850 and UFRGS-PV-0152-T (*F. tenax*) show a diploe architecture with a central cancellous core bordered by two compact cortices. Furthermore, although thin sections of another specimen of *S. galilei* [PVL 2198] were not included in our sample, observation of broken surfaces reveals the presence of a diploe structure. When present, the cancellous bone commonly occupies the core area of the osteoderm. However, in PVL 3850 (*F. tenax*), the cancellous bone also extends toward the external surface, almost reaching the tip of the external ridge of the osteoderm. Osteoderms with a compact structure have a less vascularized cortex surrounded by a more vascularized core. As observed in UFRGS-PV0629T (*P. chiniquensis*), in which thin sections and broken surfaces of caudal and dorsal osteoderms reveal a compact structure, the osteoderm microanatomy appears to be invariable along the whole row of dermal armor in each single specimen (both caudal and dorsal osteoderms show a compact structure).

3.2.2. Cortical bone

The cortical bone in all the sampled osteoderms is mostly composed of primary (non-remodeled) parallel-fibred bone tissue (Figs. 4 and 5). This highly birefringent bone tissue contains flattened and elongated bone cell lacunae, usually oriented parallel to the intrinsic fibers (Fig. 4(A, B)). Communicating canaliculi between the cell lacunae are often found. The histological differences observed among the specimens are related with the amount of vascularization and, to a lesser degree, with the arrangement of the intrinsic fibers. The amount of vascularization in the cortical bone grades from avascular (Fig. 4(A, B)) to well-vascularized (Fig. 4(C, D)), but poor vascularization is the most common observed pattern (Fig. 4(E–H)). When the external cortex is well vascularized, primary osteons or simple vascular canals are longitudinally and circumferentially arranged (although some oblique and radial anastomoses are also observable). Although the external cortex of all the samples is mainly composed of homogeneous, fine parallel-fibred bone tissue, some differences are present in UFRGS-PV-0152-T. In this specimen, the bone matrix of the external cortex is composed of a combination of parallel-fibred tissue and networks of over-crossing mineralized fiber bundles (Fig. 4(H)). Also, the basal cortex of this specimen contains coarse fibers oriented in different directions (Fig. 5(A, B)). When these fibers are transversally sectioned, each single fiber is delineated by a fine bright line.

Sharpey's fibers are observed in the whole cortical bone of all specimens. In the external cortex, Sharpey's fibers are fine and short, parallel to each other and they cross the external bone surface approximately perpendicularly (Fig. 4(E–G)). In some specimens (e.g., UFRGS-PV0629T [*P. chiniquensis*]), the spatial density of Sharpey's fibers in the external cortex is so high that they tend to blur the type of bone tissue in which they are imbedded – but not so dense as described by Vickaryous and Hall (2006) for the Sharpey's fiber bone in the osteoderms of the nine-banded armadillo, *Dasypus novemcinctus*. Sharpey's fibers located in the external cortex of UFRGS-PV0156T (*P. chiniquensis*) are regularly, but not densely arranged; they only can be observed under polarized light. At the basal cortex, Sharpey's fibers are long and they insert at sharp angles toward the marginal cortex, whereas they insert more perpendicularly to the bone surface at the middle region (Fig. 5(C–F)). Sharpey's fibers are well developed in the marginal areas of cortex (Fig. 5(G–H)). These extrinsic fibers are particularly more abundant and densely arranged in the medial cortex of the paired (precaudal) osteoderms.

Cyclic growth marks (LAGs) are well developed in the cortex of all sampled osteoderms, although their number is variable among the different specimens (Table 2). The maximum number of LAGs (15) is recorded in PVSJ 32 (*S. galilei*). The individual thickness of zones between LAGs commonly decreases toward the outer surface. In addition, the distance between two successive marks is always greater at the lateral portion of the osteoderm.

3.2.3. Internal core

The internal region of the non-remodeled specimens (e.g., UFRGS-PV0629T [*P. chiniquensis*]) consists of a well-vascularized core in which the intrinsic fibers exhibit important variations (even in the same specimen), ranging from coarse, parallel-fibred to woven-fibred bone tissues. For example, in UFRGS-PV0629T (*P. chiniquensis*), the internal core is composed of a mixture of woven and parallel-fibred bone tissue. These different bone types are not uniformly distributed in this sample. Also, non-remodeled areas in the internal core of UFRGS-PV-0152-T as well as PVL 3850 (*F. tenax*) reveal the presence of woven bone and primary osteons (fibrolamellar complex; Fig. 6(A–D)). Vascular spaces are mostly longitudinally and circumferentially arranged. Bone cell lacunae are abundant in this region; they have elongated or irregular shapes. No mineralized structural fibers (*sensu* Scheyer and Sander, 2004) were recorded in the study sample.

The internal core is always more vascularized than the cortical bone. Vascularization consists of simple vascular canals, primary osteons, or erosion cavities. In addition, remodeling processes lead to the formation of secondary osteons (Fig. 6 (C, D)). Primary vascular canals are mostly longitudinally oriented (parallel to the antero-posterior axis of the element), but radial and circumferential orientations are also present. Some anastomoses are observable toward the marginal regions (Fig. 5(G)).

In the osteoderms with a diploe microanatomy, the internal core consists of cancellous bone tissue. The cancellous bone is secondary in origin, with erosion cavities bordered by lamellar bone tissue and well-defined cementing lines. In UFRGS-PV-0152-T, although the cancellous bone is well developed, remains of primary bone tissue are observed in some non-remodeled areas of the internal core (Fig. 6(B)). The most remodeled sample corresponds to UFRGS-PV0156T (*P. chiniquensis*), in which the bony trabeculae are composed of heavily remodeled bone tissue, with no trace of primary matrix (Fig. 6(E)). These bony trabeculae exhibit lamellar tissue remnants from previous generations of secondary reconstruction. Elongated and flattened bone cell

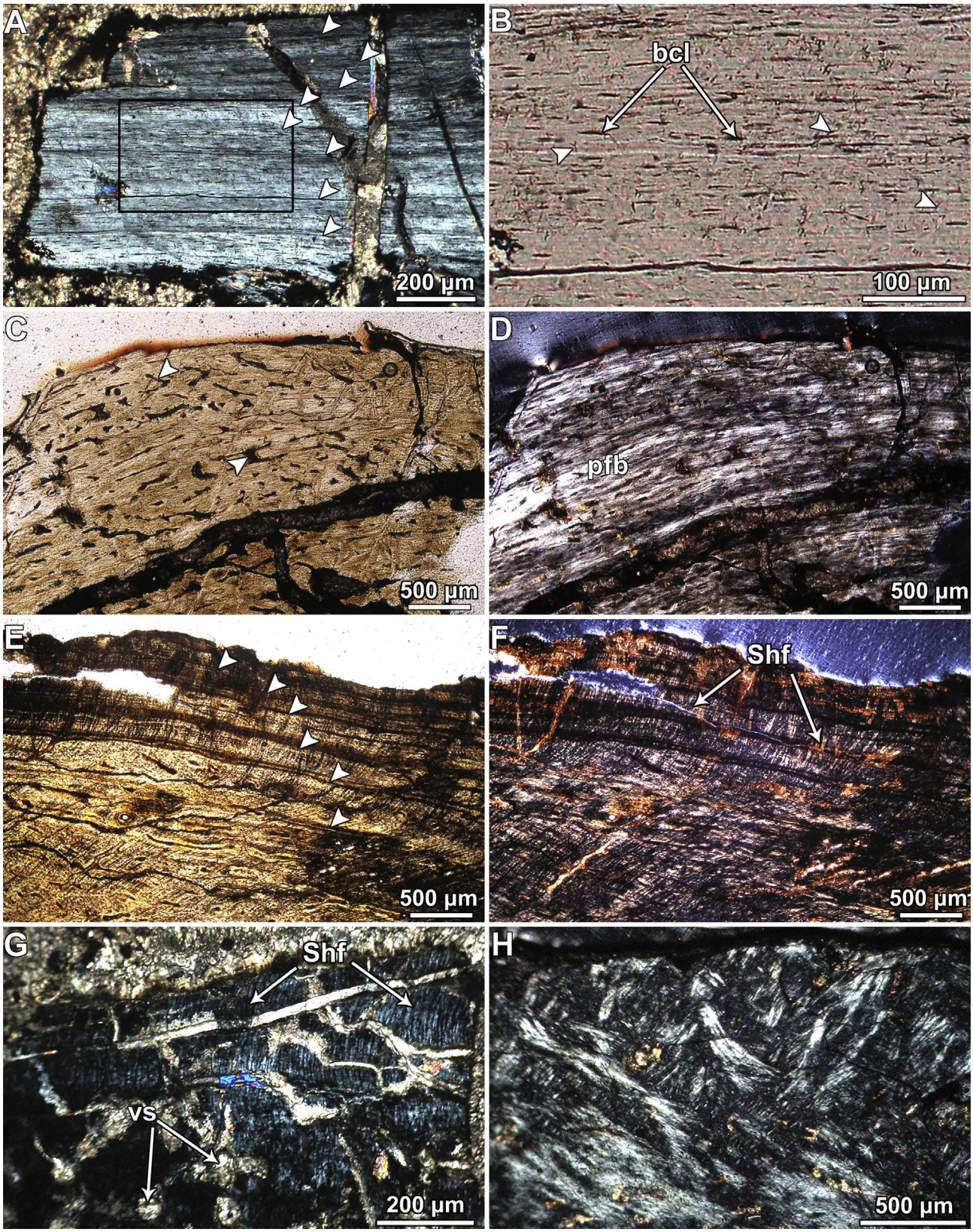

Fig. 4. External cortex histology of *Prestosuchus chiniquensis* (UFRGS-PV0156T; **A**, **B**), *Fasolasuchus tenax* (PVL 3850; **C**, **D**), *Saurosuchus galilei* (PVSJ 32; **E**, **F**), *P. chiniquensis* (UFRGS-PV0156T; **G**), and a "Rauisuchia" indet. (UFRGS-PV-0152-T; **H**). A. Cortical bone viewed under polarized light showing several LAGs (arrowheads). Note the high birefringence of parallel-fibred bone tissue. B. Close-up of the cortical bone in normal light (box inset in A) showing the flattened and elongated bone cell lacunae. Note the presence of some preserved canaliculi (arrowheads). C, D. Cortical bone viewed under normal (C) and polarized (D) light. Arrowheads indicate some radial anastomosis. E, F. External cortex viewed under normal (E) and polarized (F) light. Several LAGs (arrowheads) are visible in the outermost region. G. Detail of the cortical bone viewed under polarized light. Sharpey's fibers are abundant and they are aligned perpendicularly to the external surface. H. Cortical bone composed of networks of interwoven and mineralized fiber bundles (polarized light). Abbreviations: bcl: bone cell lacunae; pfb: parallel-fibred bone; Shf: Sharpey's fibers; vs: vascular spaces.

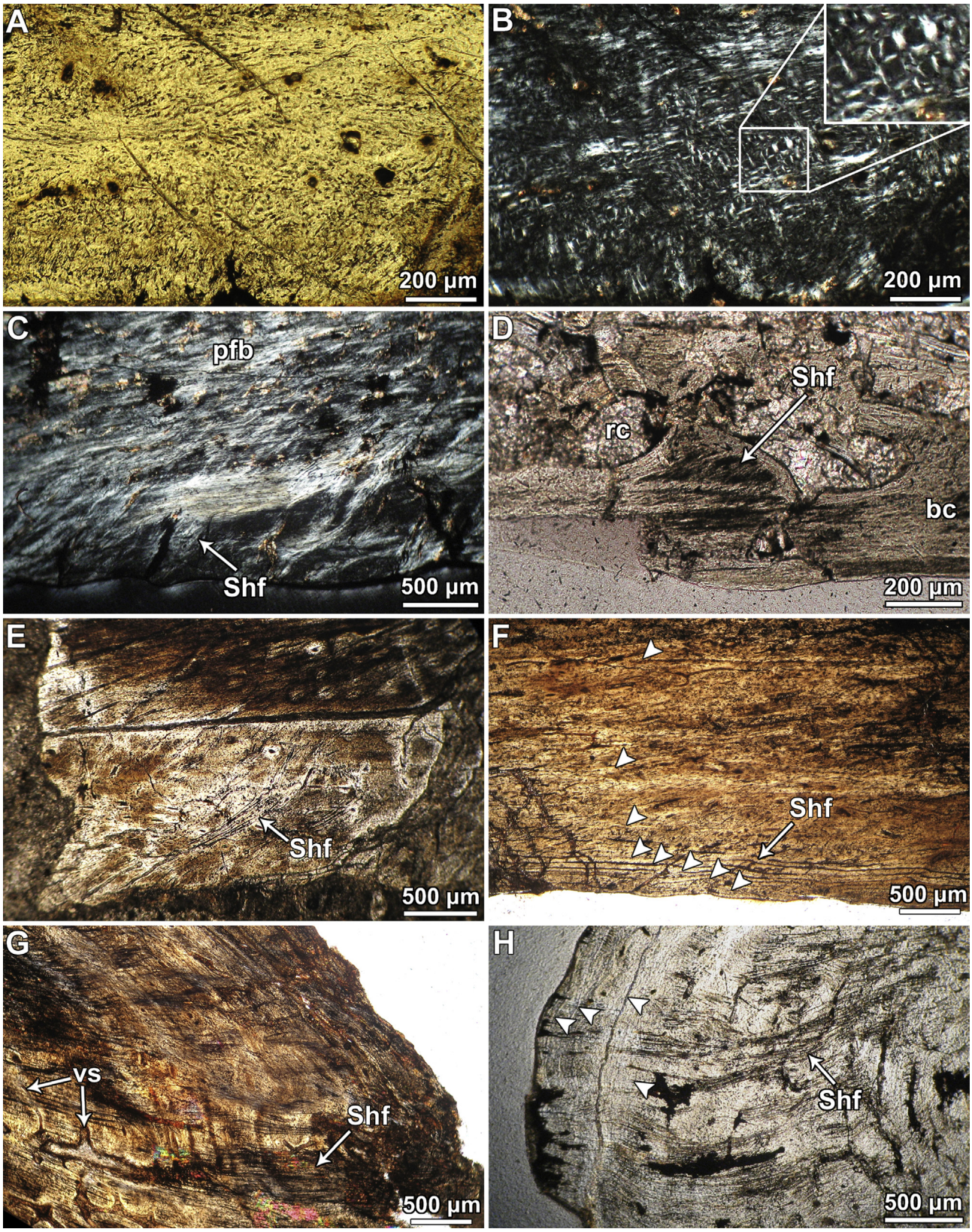

Fig. 5. Basal and marginal cortex histology of a "Rauisuchia" indet. (UFRGS-PV-0152-T; **A–C**, **H**), *Prestosuchus chiniquensis* (UFRGS-PV0156T; **D**), *P. chiniquensis* (CPEZ-239b; **E**), and *Saurosuchus galilei* (PVSJ 32; **F**, **G**). A, B. Close-up of the basal cortex viewed under normal (A) and polarized (B) light. Upper right corner in B: same tissue at higher magnification, showing coarse parallel-fibred bone whose fibers have been transversally sectioned. Note the fine white lines delineating each single fiber. C. Detail of the parallel-fibred bone and Sharpey's fibers in the basal cortex (polarized light). D. Detail of the transition between the cancellous bone of the internal core and the compact bone of the basal cortex. Note the abundance of Sharpey's fibers in the basal cortex. E. Large and fine Sharpey's fibers at the basal cortex (normal light). F. Poorly vascularized cortical bone viewed under normal light. Arrowheads indicate the presence of LAGs. G. Marginal cortex viewed under normal light. Note the radial anastomosis in the innermost region (lower left area of the image). H. Detail of the marginal cortex (normal light). Arrowheads indicate the presence of LAGs. As in G, Sharpey's fibers are abundant in this area. Abbreviations: bc: basal cortex; pfb: parallel-fibred bone; rc: resorption cavity; Shf: Sharpey's fibers; vs: vascular spaces.

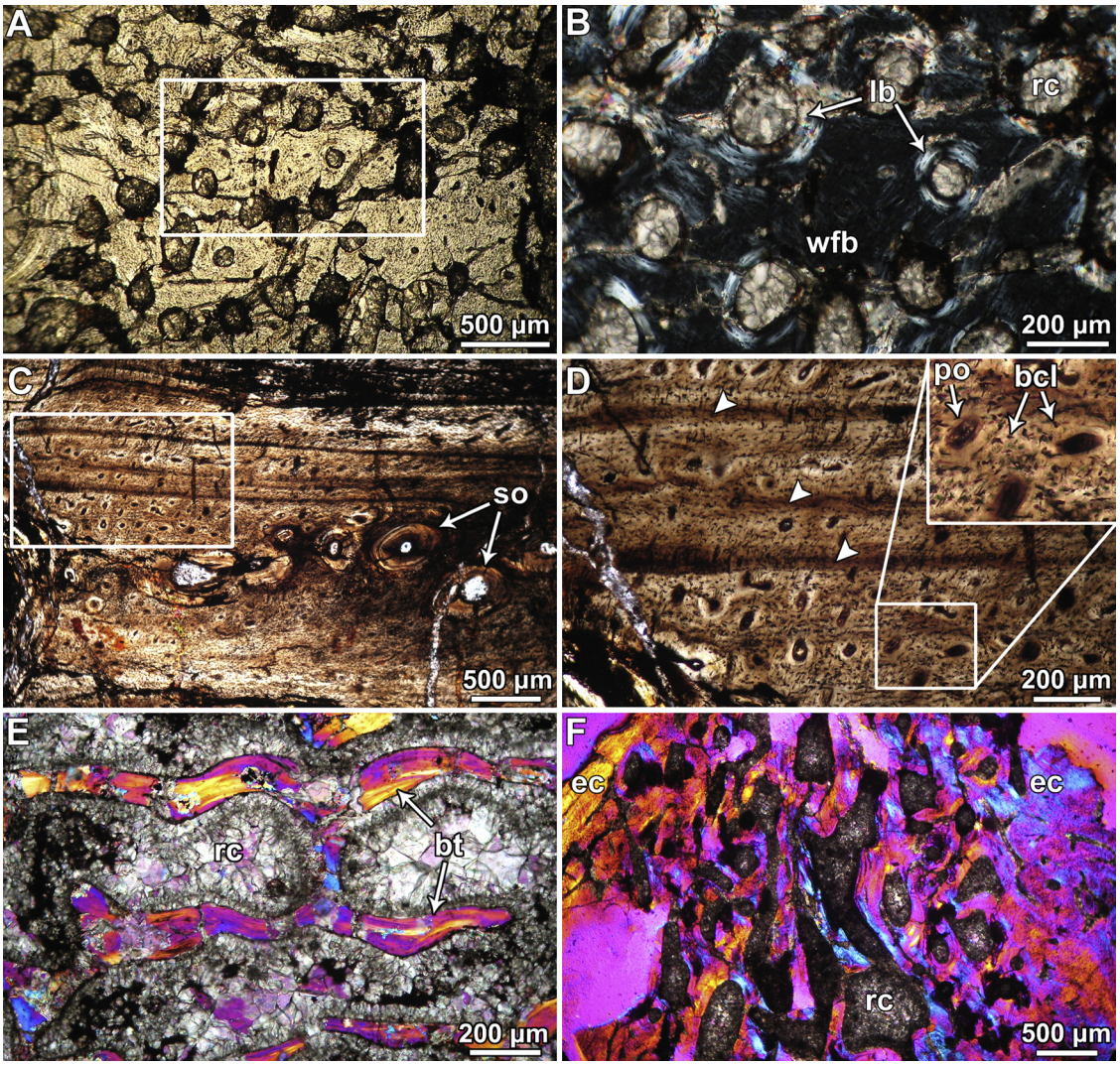

Fig. 6. Internal core histology of a "Rauisuchia" indet. (UFRGS-PV-0152-T; **A**, **B**), *Saurosuchus galilei* (PVSJ 32; **C**, **D**), *Prestosuchus chiniquensis* (UFRGS-PV0156T; **E**), and *Fasolasuchus tenax* (PVL 3850; **F**). A. Overview of partially remodeled internal core (normal light). B. Close-up of the same specimen (box inset in A) viewed under polarized light. Note the presence of monorefringent, woven-fibred bone tissue in the non-remodeled areas. C. Internal core viewed under normal light. Some secondary osteons are observed in the innermost area. D. Detailed view of the same specimen (box inset in C). LAGs are indicated by arrowheads. Upper right corner in D: same tissue at higher magnification showing bone cell lacunae and primary osteons. E. Cancellous bone of the internal core viewed under polarized light with lambda compensator. The bony trabeculae are composed of secondary lamellar bone tissue. F. Cancellous bone tissue developed toward the external cortex (polarized light with lambda compensator). Note the elongated shape of the resorption cavities. Abbreviations: bt: bony trabeculae; bcl: bone cell lacunae; ec: external cortex; lb: lamellar bone tissue; po: primary osteons; rc: resorption cavity; so: secondary osteons; wfb: woven-fibred bone tissue.

lacunae following the direction of the lining bone lamellae are observed within the trabeculae. In PVL 3850 (*F. tenax*), the cancellous bone reaches the outer cortex in the region of the ridge. Resorption cavities at this position exhibit an elongated shape (Fig. 6(F)).

4. Discussion

4.1. Bone microanatomy

A significant variation recorded in the "rauisuchian" osteoderms examined herein lies in their bone microanatomy. Whereas some specimens exhibit a distinct tri-laminar organization (diploe), others show a rather compact structure. This variation does not appear to reflect microanatomical changes related to the topographic location on body (e.g., both caudal and precaudal osteoderms of UFRGS-PV0629T [*P. chiniquensis*] show a compact structure). Also, because the osteoderms of *P. chiniquensis* can exhibit either a compact (UFRGS-PV0629T and CPEZ-239b) or a diploe structure (UFRGS-PV0156T), differences in the degree of remodeling do not appear to be related to interspecific variation among rauisuchians.

A possible explanation for the variation in the amount of cancellous bone is related to the age of the sampled specimens. If the formation of cancellous bone is a time-dependent process in rauisuchian osteoderms, more remodeled elements would correspond to older individuals. This hypothesis is supported by the relation between body size and cancellous bone development in *P. chiniquensis* and *S. galilei*. In both taxa, while cancellous bone is absent in the smaller specimens, a well-developed diploe structure is present in the larger ones (although thin sections of the larger specimen of *S. galilei* [PVL 2198] were not included in our sample, observation of broken surfaces reveals the presence of a diploe structure). If differences in body size reflect differences in age, the greater development of cancellous bone in the larger individual can possibly be related to its age.

Additionally, the recorded microanatomical variation may also reflect the sex and reproductive status of the sampled individuals. In osteoderms of extant crocodiles, internal remodeling is more intensive in breeding females, in which large amounts of minerals must be mobilized for the formation of eggshells (Hutton, 1986; Tucker, 1997; Klein et al., 2009). In rauisuchian osteoderms, the development of an internal core of cancellous bone tissue in some individuals could be interpreted as the result of mineral mobilization in females during the breeding season. Hence, specimens UFRGS-PV-0152-T, PVL 3850 and UFRGS-PV0156T could be reproductive females. The age and the reproductive status of the specimens are not mutually exclusive factors, and they together may be possibly related to the variation in the development of cancellous bone in rauisuchian osteoderms.

4.2. Histogenesis

Although fossil material does not allow direct observation of the ossification process, the structure of the resulting primary bone tissue provides hints about its formation. Studies on living taxa reveal that osteoderms found in tetrapods may be formed through metaplastic ossification, as in most reptiles (Moss, 1972; Zylberberg and Castanet, 1985; Levrat-Calviac and Zylberberg, 1986; Vickaryous and Hall, 2008), intramembranous ossification, as in the xenarthran *D. novemcinctus* (Vickaryous and Hall, 2006), or a combination of different processes (Reid, 1996; Vickaryous and Sire, 2009; Buffrénil et al., 2011). Metaplastic ossification is a process in which a pre-existing, fully-developed tissue is transformed into bone (Haines and Mohuiddin, 1968). In fossil taxa, a metaplastic origin for osteoderms has been inferred from the presence of interwoven bundles of mineralized collagen fibers with a well-ordered fiber bundle arrangement (mineralized structural fibers *sensu* Scheyer and Sander, 2004). Metaplastic development has also been proposed for osteoderm origin in anamniote tetrapods (Witzmann and Soler-Gijón, 2008; Buchwitz et al., 2012), thyreophoran and sauropod dinosaurs (Reid, 1996; Scheyer and Sander, 2004; Main et al., 2005; Cerda and Powell, 2010), some xenarthrans (Hill, 2006), as well as for the dermal bones of the turtle shell (Scheyer and Sánchez-Villagra, 2007; Scheyer and Sander, 2007; Scheyer et al., 2007, 2008). On the other hand, in an intramembranous ossification, the newly-formed osseous tissue displaces the preformed soft tissue structures instead of incorporating them. Based on the absence of mineralized structural fibers, this kind of ossification has been proposed for different extinct taxa, including some basal tetrapods (Buchwitz et al., 2012), pareiasaurs (Scheyer and Sander, 2009) and "aetosaurine" aetosaurs (Cerda and Desojo, 2011). In the case of the latter, the particular distribution of the primary bone tissues was also interpreted as independent evidence for an intramembranous origin. The lack of mineralized structural fibers and the presence of woven-fibred and fibrolamellar bone tissue in the internal core of the rauisuchian osteoderms studied by Scheyer and Desojo (2011) (except for *B. kupferzellensis*) were interpreted as evidence of intramembraneous ossification in at least some members of this group. Following this reasoning, the presence of woven-fibred bone in our sample supports the previous hypothesis of Scheyer and Desojo (2011) of an intramembraneous ossification.

However, the preserved portions of primary bone in the internal core are not entirely composed by woven-fibred bone (as in *D. novemcinctus* and "aetosaurine" aetosaurs), but also by coarse parallel-fibred bone tissue. This kind of bone tissue is also present in both external and basal cortices and appears to be related with coarse collagenous fibers incorporated by metaplasia throughout osteoderm development. Our results indicate that the rauisuchian osteoderms could originate from a complex mechanism that involves both metaplastic and intramembraneous ossifications. This kind of ossification has been previously proposed by Main et al. (2005) for the osteoderm origin in some thyreophoran dinosaurs, including *Stegosaurus*.

4.3. Growth marks and individual age

In osteoderms of extant reptiles, the growth marks (annuli and/or LAGs) are related with annual interruptions or phases of reduced bone deposition during the whole individual growth (Hutton, 1986; Tucker, 1997; Erickson and Brochu, 1999; Erickson et al., 2003). This association has been previously used for age estimation (minimum or absolute) in fossil archosaurs, including crocodilians (Erickson and Brochu, 1999; Hill and Lucas, 2006) and aetosaurs (Parker et al., 2008; Cerda and Desojo, 2011). Assuming that the preserved growth marks (LAGs) in rauisuchian osteoderms were annually deposited, the age of individuals could be determined by counting the number of these marks in the cortical bone.

In our sample, an absolute age estimation of the individuals only can be carried out in those specimens with minimal internal remodeling. The lack of intensive secondary remodeling in specimens UFRGS-PV0629T and CPEZ-239b (*P. chiniquensis*) and PVSJ 32 (*S. galilei*) implies that all counted LAGs represent the complete set of growth marks formed in an osteoderm during an individual's life-time. Given that extant crocodilians ossify their osteoderms almost one year after hatching (Chiappe et al., 1998; Vickaryous and Hall, 2008), we hypothesize that one more year have to be added to the estimated age for a more accurate determination. Hence, the estimated ages for specimens CPEZ-239b, UFRGS-PV0629T, and PVSJ 32 are 6, 8 and 16 years, respectively. As in the case of the other sampled specimens, the estimated age obtained from this method is necessarily a minimum age because of secondary remodeling of the internal core, which is particularly extensive in UFRGS-PV0156T. Scheyer and Desojo (2011) proposed that rauisuchian osteoderms appear to be well suited to infer absolute age in these archosaurs. Our data indicate that it is true only in those specimens where the secondary remodeling of the internal core is minimal or absent.

4.4. Systematic value

Osteoderm microstructure has been demonstrated to be a valuable tool for systematics in different amniote groups (Scheyer and Sander, 2004; Hill, 2006; Scheyer and Sánchez-Villagra, 2007; Burns, 2008; Wolf et al., 2011). For instance, Scheyer and Sander (2004) found that the density and arrangements of the collagen fibers and the microanatomy differ in ankylosaurian dinosaurs and allow for differentiation between three major groups. Concerning rauisuchian osteoderms, although microstructural variation is reported here as well as in the study of Scheyer and Desojo (2011), such variation does not appear to be related to systematic differences among taxa. First, as previously discussed, the reported differences in the microanatomy (compact *vs.* diploe) appear instead to be related to the age, sex and reproductive stage of the individuals. The presence of mineralized structural fibers originated by metaplasia in the core region of *B. kupferzellensis* (Scheyer and Desojo, 2011) is perhaps the only histological feature with taxonomic value among rauisuchians, because this character has only been reported in this taxon.

4.5. Comparison with other pseudosuchian taxa

The data obtained from our sample and from the study of Scheyer and Desojo (2011) allow us to compare the osteoderm microstructure of rauisuchians with other pseudosuchian taxa, specifically Aetosauria and Crocodylomorpha. Since the internal

microanatomy of rauisuchians is variable even within a single taxon, we only compare their fine histology. The deep cortex of pseudosuchians is commonly composed of parallel-fibred bone tissue (Hill and Lucas, 2006; Scheyer and Sander, 2004; Parker et al., 2008; Vickaryous and Hall, 2008; Vickaryous and Sire, 2009; Hill, 2010; Klein et al., 2009; Cerda and Desojo, 2011; Scheyer and Desojo, 2011). In rauisuchians and crocodylomorphs, the internal cortex (when not remodeled) is composed of parallel-fibred, woven-fibred, and fibrolamellar bone tissues. In some taxa, mineralized structural fiber bundles have been also reported in this region (Hill and Lucas, 2006; Scheyer and Sander, 2004; Vickaryous and Hall, 2008; Vickaryous and Sire, 2009; Klein et al., 2009; Cerda and Desojo, 2011; Scheyer and Desojo, 2011). On the other hand, the internal core of aetosaurian paramedian osteoderms mainly consists of fibrolamellar bone tissue (Cerda and Desojo, 2011). Also, the fibrolamellar bone in aetosaurian osteoderms has a particular distribution within the osteoderm, which has not been reported before for rauisuchians and crocodylomorphs. As was mentioned for the notosuchian crocodylomorph *Simosuchus clarki* (Hill, 2010), the superficial cortex of the rauisuchian osteoderms does not reveal any process of resorption and new deposition of periosteal bone. This observation contrasts with that reported for aetosaurs (Cerda and Desojo, 2011) and several crocodylomorph taxa (Buffrénil, 1982; Scheyer and Sander, 2004), where the superficial cortex reveals a continuous process of resorption and re-deposition of the bone tissue, which also includes preferential bone deposition in some particular sites. This process of resorption and re-deposition is evident in taxa where osteoderms possess a strong ornamentation (deep pits and grooves), but is absent in elements with a delicate external ornamentation (e.g., rauisuchians). Hence, this histological variation is possibly related to the degree of ornamentation of the superficial surface.

The distribution of Sharpey's fibers is another histological feature that can be compared between different pseudosuchian taxa. While Sharpey's fibers are well developed in the deep and marginal cortices of rauisuchian and crocodylomorph osteoderms, these extrinsic fibers are mostly restricted to the marginal cortex (lateral and medial cortices) in aetosaurs (Hill and Lucas, 2006; Scheyer and Sander, 2004; Klein et al., 2009; Scheyer and Desojo, 2011; Cerda and Desojo, 2011). Cerda and Desojo (2011) hypothesized that the particular distribution of Sharpey's fibers in aetosaurian osteoderms is related to the bond between adjacent osteoderms in a single file. If the same would be the case in the precaudal osteoderms of rauisuchians (caudal osteoderms are not paired), an asymmetrical distribution of Sharpey's fibers would be expected (a major density of fibers in the medial cortex). However, we do not observe such an asymmetrical pattern in the cervical osteoderm of PVSJ 32 (*S. galilei*), the only precaudal osteoderm for which the lateral and medial cortices are well preserved. The absence of parasagittal sections in our sample precludes identification of Sharpey's fibers related to the presence of an interosteodermal ligament between adjacent osteoderms in a row (Salisbury and Frey, 2000; Buchwitz et al., 2012).

Overall, the osteoderm histology of rauisuchians appears to be more similar to crocodylomorphs than to aetosaurs. Our data support the recent phylogenetic study of Nesbitt (2011), in which all rauisuchian taxa considered here are on the stem leading to Crocodylomorpha (Loricata). This contrasts with the phylogenetic hypothesis of Brusatte et al. (2010), in which aetosaurs are among the closest relatives of crocodylomorphs. Nevertheless, given the still limited information related to osteoderm microstructure in pseudosuchians, the inferences with regard to the state and distribution of histological characters (e.g., identification of ancestral characters in Pseudosuchia) and their influence for phylogenetic studies must be treated with caution.

5. Conclusions

This study expands our knowledge regarding the morphology and histology of rauisuchian osteoderms, supporting previously-obtained results, but also providing new data on different issues. First, we recognize intra-specific variations in osteoderm microanatomy that were not previously reported, possibly related to the age, sex and reproductive status of the individuals. The value of osteoderms for age estimation only appears to be reliable in specimens where secondary remodeling is absent or minimal. With regards to the origin and development of the osteoderm, our data agree with the previously proposed process of intramembraneous ossification, but also suggest that other mechanisms (e.g., metaplasia) were also possibly involved. Finally, the microstructure of osteoderms does not appear to be useful for systematic analyses within rauisuchians. Nevertheless, if the number of sampled pseudosuchian taxa is increased in the future, the osteoderm microstructure could become a valuable tool in higher taxonomic comparisons.

Acknowledgements

We thank J. Powell (PVL) and R. Martinez (UNSJ) who allowed us to study specimens under their care; D. Codega for the skilful preparation of the histological sections; J. González for the *Prestosuchus chiniquensis* reconstruction in Fig. 1; J. Trotteyn, M. Lacerda, and B. von Baczko for their cooperation and support with the pictures and transportation of the specimens; and M. Buchwitz, V. de Buffrénil, W. Parker and an anonymous reviewer for constructive suggestions that improved this manuscript. This research was partially funded by the Agencia Nacional de Promoción Científica y Técnica PICT 2010 No. 207 (to I.A.C. and J.B.D.) and by Swiss National Science Foundation No. 31003A 127053 (to T.M.S.).

References

Alcober, O., 2000. Redescription of the skull of *Saurosuchus galilei* (Archosauria: Rauisuchidae). Journal of Vertebrate Paleontology 20, 302–316.

Azevedo, S.A.K., 1991. *Prestosuchus chiniquensis* Huene 1942 (Reptilia, Archosauria, Thecodontia, Proterosuchia, Rauisuchidae), da Formação Santa Maria, Triássico do Estado do Rio Grande do Sul, Brasil. Ph.D. thesis, Universidade Federal do Rio Grande do Sul (unpublished).

Barberena, M.C., 1978. A huge thecodont skull from the Triassic of Brazil. Pesquisas 7, 111–129.

Bonaparte, J.F., 1981. Descripción de *Fasolasuchus tenax* y su significado en la sistemática y evolución de los Thecodontia. Revista del Museo Argentino de Ciencias Naturales Bernardino Rivadavia 3, 55–101.

Brusatte, S.L., Benton, M.J., Desojo, J.B., Langer, M.C., 2010. The higher level phylogeny of Archosauria (Tetrapoda: Diapsida). Journal of Systematic Palaeontology 8, 3–47.

Buchwitz, M., Witzmann, F., Voigt, S., Golubev, V., 2012. Osteoderm microstructure indicates the presence of a crocodylian-like trunk brancing system in a group of armoured basal tetrapods. Acta Zoologica (Stockholm) 93, 260–280.

de Buffrénil, V., 1982. Morphogenesis of bone ornamentation in extant and extinct crocodilians. Zoomorphology 99, 155–166.

de Buffrénil, V., Farlow, J., de Ricqlès, A., 1986. Growth and function of *Stegosaurus* plates: evidence from bone histology. Paleobiology 12, 459–473.

de Buffrénil, V., Dauphin, Y., Rage, J.C., Sire, J.Y., 2011. An enamel-like tissue, osteodermine, on the osteoderms of a fossil anguid (Glyptosaurinae) lizard. Comptes Rendus Palevol 10, 427–437.

Burns, M.E., 2008. Taxonomic utility of ankylosaur (Dinosauria, Ornithischa) osteoderms: *Glyptodontopelta mimus* Ford, 2000: a test case. Journal of Vertebrate Paleontology 28, 1102–1109.

Cerda, I.A., Desojo, J.B., 2011. Dermal armour histology of aetosaurs (Archosauria: Pseudosuchia), from the Upper Triassic of Argentina and Brazil. Lethaia 44, 417–428.

Cerda, I.A., Powell, J.E., 2010. Dermal armor histology of *Saltasaurus loricatus*, an Upper Cretaceous sauropod dinosaur from Northwest Argentina. Acta Palaeontologica Polonica 55, 389–398.

Chinsamy, A., Raath, M.A., 1992. Preparation of fossil bone for histological examination. Palaeontologia Africana 29, 39–44.

Chiappe, L.M., Coria, R.A., Dingus, L., Jackson, F., Chinsamy, A., Fox, M., 1998. Sauropod dinosaur embryos from the Late Cretaceous of Patagonia. Nature 396, 258–261.

Desojo, J.B., Ezcurra, M.D., Schultz, S.L., 2011. An unusual new archosauriform from the Middle–Late Triassic of southern Brazil and the monophyly of Doswelliidae. Zoological Journal of the Linnean Society 161, 839–871.
Dias, E.V., Richter, M., 2002. On the squamation of *Australerpeton cosgriffi* Barberena, a temnospondyl amphibian from the Upper Permian of Brasil. Anais da Academia Brasileira de Ciências 74, 477–490.
Erickson, G.M., Brochu, C.M., 1999. How the 'terror crocodile' grew so big. Nature 398, 205–206.
Erickson, G.M., de Ricqlès, A., de Buffrénil, V., de Molnar, R.E., Bayless, M.K., 2003. Vermiform bones and the evolution of gigantism in *Megalania*–how a reptilian fox became a lion. Journal of Vertebrate Paleontology 23, 966–970.
Farlow, J.O., Hayashi, S., Tattersall, G.J., 2010. Internal vascularity of the dermal plates of *Stegosaurus* (Ornithischia, Thyreophora). Swiss Journal of Geosciences 103, 173–185.
França, M.A.G., Ferigolo, J., Langer, M.C., 2011. Associated skeletons of a new middle Triassic Rauisuchia from Brazil. Naturwissenschaften 98, 389–395.
Francillon-Vieillot, H., de Buffrénil, V., Castanet, J., Géraudie, J., Meunier, F.J., Sire, J.Y., Zylberberg, L., de Ricqlès, A., 1990. Microstructures and mineralization of vertebrate skeletal tissues. In: Carter, J. (Ed.), Skeletal biomineralizations: patterns, processes and evolutionary trends 1. Van Nostrand Reinhold, New York, pp. 471–530.
Gower, D.J., 2000. Rauisuchian archosaurs (Reptilia, Diapsida): an overview. Neues Jahrbuch für Geologie und Paläontologie, Abhandlungen 218, 447–488.
Haines, R.W., Mohuiddin, A., 1968. Metaplastic bone. Journal of Anatomy 103, 527–538.
Hayashi, S., Carpenter, K., Scheyer, T.M., Watabe, M., Suzuki, D., 2010. Function and evolution of ankylosaur dermal armor. Acta Palaeontologica Polonica 55, 213–228.
Hill, R.V., 2006. Comparative anatomy and histology of xenarthran osteoderms. Journal of Morphology 267, 1441–1460.
Hill, R.V., 2010. Osteoderms of *Simosuchus clarki* (Crocodyliformes: Notosuchia) from the Late Cretaceous of Madagascar. Journal of Vertebrate Paleontology Memoir 10, 154–176.
Hill, R.V., Lucas, S.G., 2006. New data on the anatomy and relationships of the Paleocene crocodylian *Akanthosuchus langstoni*. Acta Palaeontologica Polonica 51, 455–464.
Hua, S., de Buffrénil, V., 1996. Bone histology as a clue in the interpretation of functional adaptations in the Thalattosuchia (Reptilia, Crocodylia). Journal of Vertebrate Paleontology 16, 703–717.
von Huene, F., 1938. Die fossilen Reptilien des südamerikanischen Gondwanalandes. Neues Jahrbuch für Mineralogie. Geologie und Paläontologie 1938, 142–151.
Hutton, J.M., 1986. Age determination of living Nile crocodiles from the cortical stratification of bone. Copeia 1986, 332–341.
Klein, N., Scheyer, T.M., Tütken, T., 2009. Skeletochronology and isotopic analysis of a captive individual of *Alligator mississippiensis* Daudin, 1802. Fossil Record 12, 121–131.
Krebs, B., 1965. Die Triasfauna der Tessiner Kalkalpen.XIX. *Ticinosuchus ferox*, nov. gen. nov. sp. Ein neuer Pseudosuchier aus der Trias des Monte San Georgio. Schweizersiche Paläontologische Abhandlungen 81, 1–140.
Lacerda, M.B., 2012. Descrição e estudo de novos espécimes de Prestosuchus chiniquensis (Archosauria, Rauisuchia) do afloramento Sanga da Árvore, Municipio de São Pedro do Sul, Região deXiniquá. Estado do Rio Grande do Sul. Brasil. Master Thesis, Universidade Federal do Rio Grande do Sul (unpublished).
Lacerda, M.B., Schultz, S.L., 2010. A probable juvenile of *Prestosuchus chiniquensis* (Archosauria, Rauisuchia) from the Sanga da Árvore Site, Chiniquá Region, Rio Grande do Sul State, Brazil. VII Simpósio Brasileiro de Paleontologia de Vertebrados, Julho de 2010 Paleontologia em Destaque. Edição Especial.
Levrat-Calviac, V., Zylberberg, L., 1986. The structure of the osteoderms in the gekko: *Tarentola mauritanica*. The American Journal of Anatomy 176, 437–466.
Main, R.P., de Ricqlès, A., Horner, J., Padian, K., 2005. The evolution and function of thyreophoran dinosaur scutes: implications for plate function in stegosaurs. Paleobiology 31, 291–314.
Mastrantonio, B.M., 2010. Descrição osteológica de materials cranianos e pós-cranianos de *Prestosuchus chiniquensis* (Arcosauria, Rauisuchia) do mesotriássico do RS (Biozona de Dinodontosaurus, Formação Santa Maria) e considerações filogenéticas sobre os rauissúquios. Ph.D. Thesis, Universidade Federal do Rio Grande do Sul (unpublished).
Mastrantonio, B.M., Desojo, J.B., Schultz, C.L., 2008. Um novo espécime de rauissúquio (Archosauria, Reptilia) Triássico da Formação Santa Maria, Bacia do Paraná, Brasil, e suas implicações na diagnose de Prestosuchus Huene, 1938. III Congreso Latinoamericano de Paleontología de Vertebrados, Universidad Nacional del Comahue, Neuquén, Argentina. Libro de Resúmenes, p. 155.
Moss, M.L., 1972. The vertebrate dermis and the integumental skeleton. American Zoologist 12, 27–54.
Nesbitt, S.J., 2005. The osteology of the Middle Triassic pseudosuchian archosaur *Arizonasaurus babbitti*. Historical Biology 17, 19–47.
Nesbitt, S.J., 2011. The early evolution of archosaurs: relationships and the origin of major clades. Bulletin of the American Museum of Natural History 352, 1–292.
Nesbitt, S., Brusatte, S., Desojo, J.B., Liparini, A., de França, M., Weinbaum, J., Gower, D., (in press). Rauisuchia. Geological Society of London, Special Volumen: Anatomy, Phylogeny and Palaeobiology of Basal Archosaurs.
Parker, W.G., Stocker, M.R., Irmis, R.B., 2008. A new desmatosuchine aetosaur (Archosauria: Suchia) from the Upper Triassic Tecovas Formation (Dockum Group) of Texas. Journal of Vertebrate Paleontology 28, 692–701.
Reid, R.E.H., 1996. Bone histology of the Cleveland-Lloyd dinosaurs and of dinosaurs in general. Part I: Introduction to bone tissues. Brigham Young University Geology Studies 41, 25–72.
Reig, O.A., 1959. Primeros datos descriptivos sobre nuevos reptiles arcosaurios del Triásico de Ischigualasto. Revista de la Asociación Geológica Argentina 13, 257–270.
de Ricqlès, A., Pereda Suberbiola, X., Gasparini, Z., Olivero, E., 2001. Histology of the dermal ossifications in an ankylosaurian dinosaur from the Late Cretaceous of Antarctica. Asociación Paleontológica Argentina, Publicación Especial 7, 171–174.
Romer, A.S., 1971. The Chañares (Argentina) Triassic reptile fauna. VIII. A fragmentary skull of a large thecodont, *Luperosuchus fractus*. Breviora 373, 1–8.
Salisbury, S.W., Frey, E., 2000. A biomechanical transformation model for the evolution of semi-spheroidal articulations between adjoining vertebral bodies in crocodilians. In: Grigg, G.C., Seebacher, F., Franklin, C.E. (Eds.), Crocodilian Biology and Evolution. Surrey Beatty and Sons, Chipping Norton, pp. 85–134.
Scheyer, T.M., 2007. Skeletal histology of the dermal armor of Placodontia: the occurrence of 'postcranial fibro-cartilaginous bone' and its developmental implications. Journal of Anatomy 211, 737–753.
Scheyer, T.M., Brüllmann, B., Sánchez-Villagra, M.R., 2008. The ontogeny of the shell in side-necked turtles, with emphasis on the homologies of costal and neural bones. Journal of Morphology 269, 1008–1021.
Scheyer, T.M., Desojo, J.B., 2011. Palaeohistology and microanatomy of rauisuchian osteoderms (Archosauria: Pseudosuchia). Palaeontology 54, 1289–1302.
Scheyer, T.M., Sánchez-Villagra, M.R., 2007. Carapace bone histology in the giant pleurodiran turtle *Stupendemys geographicus*: phylogeny and function. Acta Palaentologica Polonica 52, 137–154.
Scheyer, T.M., Sander, P.M., 2004. Histology of ankylosaur osteoderms: implications for systematics and function. Journal of Vertebrate Paleontology 24, 874–893.
Scheyer, T.M., Sander, P.M., 2007. Shell bone histology indicates terrestrial palaeoecology of basal turtles. Proceedings of the Royal Society B 274, 1885–1893.
Scheyer, T.M., Sander, P.M., 2009. Bone microstructures and mode of skeletogenesis in osteoderms of three pareiasaurs taxa from the Permian of South Africa. Journal of Evolutionary Biology 22, 1153–1162.
Scheyer, T.M., Sander, P.M., Joyce, W.G., Böhme, W., Witzel, U., 2007. A plywood structure in the shell of fossil and living softshelled turtles (Trionychidae) and its evolutionary implications. Organisms. Diversity & Evolution 7, 136–144.
Trotteyn, M.J., Desojo, J.B., Alcober, O.A., 2011. Nuevo material postcraneano de *Saurosuchus galilei* (Archosauria: Crurotarsi) del Triásico Superior del centro-oeste de Argentina. Ameghiniana 48, 605–620.
Tucker, A.D., 1997. Validation of skeletochronology to determine age of freshwater crocodiles (*Crocodylus johnstoni*). Marine and Freshwater Research 48, 343–351.
Vickaryous, M.K., Hall, B.K., 2006. Osteoderm morphology and development in the nine-banded armadillo, *Dasypus novemcinctus* (Mammalia, Xenartha, Cingulata). Journal of Morphology 267, 1273–1283.
Vickaryous, M.K., Hall, B.K., 2008. Development of the dermal skeleton in *Alligator mississippiensis* (Archosauria, Crocodylia) with comments on the homology of osteoderms. Journal of Morphology 269, 398–422.
Vickaryous, M.K., Sire, J.Y., 2009. The integumentary skeleton of tetrapods: origin, evolution, and development. Journal of Anatomy 214, 441–464.
Witzmann, F., 2009. Comparative histology of sculptured dermal bones in basal tetrapods, and the implications for the soft tissue dermis. Palaeodiversity 2, 233–270.
Witzmann, F., Soler-Gijón, R., 2008. The bone histology of osteoderms in temnospondyl amphibians and in the chroniosuchian *Bystrowiella*. Acta Zoologica (Stockholm) 89, 1–19.
Wolf, D., Kalthoff, D.C., Sander, P.M., 2011. Osteoderm histology of the Pampatheriidae (Cingulata, Xenarthra, Mammalia): implications for systematics, osteoderm growth, and biomechanical adaptation. Journal of Morphology 273, 388–404.
Zylberberg, L., Castanet, J., 1985. New data on the structure and growth of the osteoderms in the reptile *Anguis fragilis* L. (Anguidae, Squamata). Journal of Morphology 186, 327–342.